

Cortactin deficiency causes increased RhoA/ROCK1-dependent actomyosin contractility, intestinal epithelial barrier dysfunction, and disproportionately severe DSS-induced colitis

AF Citalán-Madrid¹, H Vargas-Robles¹, A García-Ponce¹, M Shibayama², A Betanzos^{2,3}, P Nava⁴, C Salinas-Lara⁵, K Rottner^{6,7}, R Mennigen⁸ and M Schnoor¹

The intestinal epithelium constitutes a first line of defense of the innate immune system. Epithelial dysfunction is a hallmark of intestinal disorders such as inflammatory bowel diseases (IBDs). The actin cytoskeleton controls epithelial barrier integrity but the function of actin regulators such as cortactin is poorly understood. Given that cortactin controls endothelial permeability, we hypothesized that cortactin is also important for epithelial barrier regulation. We found increased permeability in the colon of cortactin-KO mice that was accompanied by reduced levels of ZO-1, claudin-1, and E-cadherin. By contrast, claudin-2 was upregulated. Cortactin deficiency increased RhoA/ROCK1-dependent actomyosin contractility, and inhibition of ROCK1 rescued the barrier defect. Interestingly, cortactin deficiency caused increased epithelial proliferation without affecting apoptosis. KO mice did not develop spontaneous colitis, but were more susceptible to dextran sulfate sodium colitis and showed severe colon tissue damage and edema formation. KO mice with colitis displayed strong mucus deposition and goblet cell depletion. In healthy human colon tissues, cortactin co-localized with ZO-1 at epithelial cell contacts. In IBDs patients, we observed decreased cortactin levels and loss of co-localization with ZO-1. Thus, cortactin is a master regulator of intestinal epithelial barrier integrity *in vivo* and could serve as a suitable target for pharmacological intervention in IBDs.

INTRODUCTION

The integrity of the epithelial monolayer is critical for healthy intestines. This monolayer constitutes a semi-permeable barrier that is tightly regulated to allow absorption of nutrients and water and at the same time restrict excessive leakage of macromolecules and invasion of bacteria from the gut lumen. Increased epithelial permeability is a characteristic of chronic inflammatory disorders such as inflammatory bowel diseases (IBDs).¹ Epithelial permeability is mostly controlled by tight junctions (TJs),² whereas stable cell-cell adhesion depends on adherens junctions (AJs).³ Together, AJs and TJs form the apical junctional complex that controls epithelial barrier

integrity.⁴ These junctional structures are composed of transmembrane adhesion receptors that are intracellularly linked to the actin cytoskeleton via adaptor molecules such as zonula occludens (ZO) and catenins.^{5,6} It is commonly accepted that proper apical junctional complex functions and thus epithelial barrier integrity in health and disease are strongly dependent on actin dynamics.^{4,7} The connection of AJs and TJs to the actin cytoskeleton is further regulated by several actin-binding molecules including cortactin.⁸

Cortactin is a multi-domain protein capable of directly binding actin filaments, other actin regulators such as the Arp2/3 complex and adaptor molecules including ZO-1.⁹

¹Department of Molecular Biomedicine, CINVESTAV-IPN, Mexico City, Mexico. ²Department of Infectomics and Molecular Pathogenesis, CINVESTAV-IPN, Mexico City, Mexico. ³Consejo Nacional de Ciencia y Tecnología, Mexico City, Mexico. ⁴Department of Physiology, Biophysics and Neurosciences, CINVESTAV-IPN, Mexico City, Mexico. ⁵Laboratory of Histology and Pathology, Faculty of Superior Studies Iztacala, UNAM, Mexico City, Mexico. ⁶Division of Molecular Cell Biology, Zoological Institute, TU Braunschweig, Braunschweig, Germany. ⁷Department of Cell Biology, Helmholtz Centre for Infection Research, Braunschweig, Germany and ⁸Clinic for General and Visceral Surgery, University Clinic of Münster, Münster, Germany. Correspondence: M Schnoor (mschnoor@cinvestav.mx)

Received 26 May 2016; accepted 18 December 2016; published online 25 January 2017. doi:10.1038/mi.2016.136

Several studies highlighted the importance of cortactin for epithelial junction stability *in vitro*. For example, cortactin is recruited to epithelial cell contacts upon homophilic E-cadherin engagement where it coordinates AJs formation and Arp2/3- and WAVE2-dependent actin remodeling.^{10,11} Cortactin also interacts and colocalizes with p120-catenin at cell-cell contacts.¹² Moreover, cortactin directly binds to ZO-1 at TJs.¹³ However, despite reports describing a decrease in epithelial junction integrity *in vitro* after downregulation of cortactin, it remains unexplored whether cortactin deficiency affects intestinal epithelial barrier functions *in vivo*. This is especially important given the fact that not all observed effects on actin dynamics after cortactin downregulation in cell lines could be reproduced in primary cortactin-deficient cells.¹⁴ Another open question is whether cortactin expression and localization is affected in IBDs patients.

Here, we addressed the physiological relevance of cortactin in the colon. We demonstrate that cortactin deficiency causes increased RhoA/ROCK1-dependent actomyosin contractility and altered molecular composition of AJs and TJs leading to increased permeability. This barrier defect is not sufficient to induce spontaneous colitis but strongly aggravates experimental colitis in cortactin-KO mice. Furthermore, in human colon tissue biopsies of individuals suffering from IBDs, we observe decreased levels of cortactin and loss of colocalization with ZO-1 at cell contacts.

RESULTS

Loss of cortactin leads to increased intestinal permeability, altered composition of junctions, and increased proliferation

Epithelial dysfunction contributes to relapsing intestinal inflammation during IBDs. For example, junctional adhesion molecule-A deficiency enhanced colonic inflammation and permeability in mice.¹⁵ On the other hand, it is known that correct actin cytoskeleton dynamics are a prerequisite for epithelial barrier integrity. However, the functions of actin regulators such as cortactin in the colon are not well studied. In a previous study, we demonstrated that cortactin deficiency caused increased endothelial permeability.¹⁶ Thus, we hypothesized that loss of cortactin also leads to increased intestinal epithelial permeability. This was indeed the case as permeability in the colon increased by $24.8 \pm 3.7\%$ under basal conditions (**Figure 1a**). However, KO mice do not appear sick by visual inspection, suggesting that hitherto unknown compensatory mechanisms may exist. Permeability is controlled by junctional adhesion molecules that are connected by adaptor molecules to the actin cytoskeleton.¹⁷ Thus, we analyzed whether the absence of cortactin would affect the expression or localization of junction molecules. As shown in **Figure 1b**, there is a significant decrease in the expression of the TJs proteins ZO-1 and claudin-1. By contrast, the expression of the pore-forming claudin-2 increased significantly in cortactin-KO colons. E-cadherin, β -catenin, and actin levels were not significantly affected when normalized to tubulin expression. Immunofluorescence studies confirmed that ZO-1 and

claudin-1 were decreased at cell contacts while claudin-2 was increased (**Figure 1c**). These findings imply that cortactin contributes to the maintenance of junction architecture and thus a stable barrier *in vivo*. We also consistently observed that epithelial crypts seemed less densely packed as manifested by an increase in the distance between epithelial nuclei (**Figure 1d**, left panel). Quantification demonstrated that the distance from the center of one nucleus to the center of the nucleus of the neighboring cell significantly increased from $6.48 \pm 0.79 \mu\text{m}$ in WT crypts to $9.98 \pm 1.27 \mu\text{m}$ in cortactin KO crypts (**Figure 1d**, right panel). However, the average number of cells that constitute a crypt was not significantly changed (data not shown), suggesting that cortactin KO crypt epithelial cells are wider than WT cells.

A correct balance between proliferation and apoptosis also contributes to a stable intestinal epithelial barrier. Interestingly, we detected increased phosphorylation of histone-H3 (**Figure 1e**), and increased expression of KI67 in epithelial cells along the crypt axes which is in WT colons restricted to the crypt base (**Figure 1f**), suggesting that cortactin deficiency triggers epithelial proliferation. Poly-(ADP-ribose)-polymerase and caspase-3 were not cleaved in both WT and KO colons (**Figure 1e**). Thus, apoptosis does not contribute to barrier destabilization without cortactin.

Cortactin deficiency aggravates experimental colitis

Given the observed barrier dysfunction in basal conditions, we speculated that cortactin deficiency might render mice more susceptible to experimental colitis. Indeed, treatment with 3.5% dextran sulfate sodium (DSS) in drinking water, a concentration tolerated by our WT littermate control mice over the usual experimental period of 7 days, induced such a severe colitis in cortactin KO animals that they had to be killed on day 5. **Figure 2a** shows that the disease activity index of KO animals with DSS was significantly higher over the entire course of the experiment starting on day 1. Visible fecal bleeding in KO mice also started as early as one day after starting the treatment. Interestingly, untreated KO mice only showed slight clinical signs of colitis supporting the notion that protective mechanisms are in place that prevent development of spontaneous colitis despite increased permeability. Weight loss was significantly higher in treated KO mice already starting on day 3 (**Figure 2b**). Both WT and KO colons were significantly shorter after 5 days of DSS treatment compared with untreated controls, but this shortening was not further increased by cortactin deficiency (**Figure 2c**). Histological analyses of colon "swiss rolls" (see **Supplementary Figure S1A** online) and magnifications of distal colon areas of the respective "swiss rolls" (**Figure 2d,e**) showed signs of edema formation in KO mice even without treatment, thus corroborating the observed increased permeability (**Figure 1a**). KO animals treated with DSS showed severe edema formation, ulcerations, and an overall loss of tissue architecture (**Figure 2d,e**). Histological scoring confirmed these observations (see **Supplementary Figure S1B**). Untreated WT mice did not show signs of tissue damage, whereas

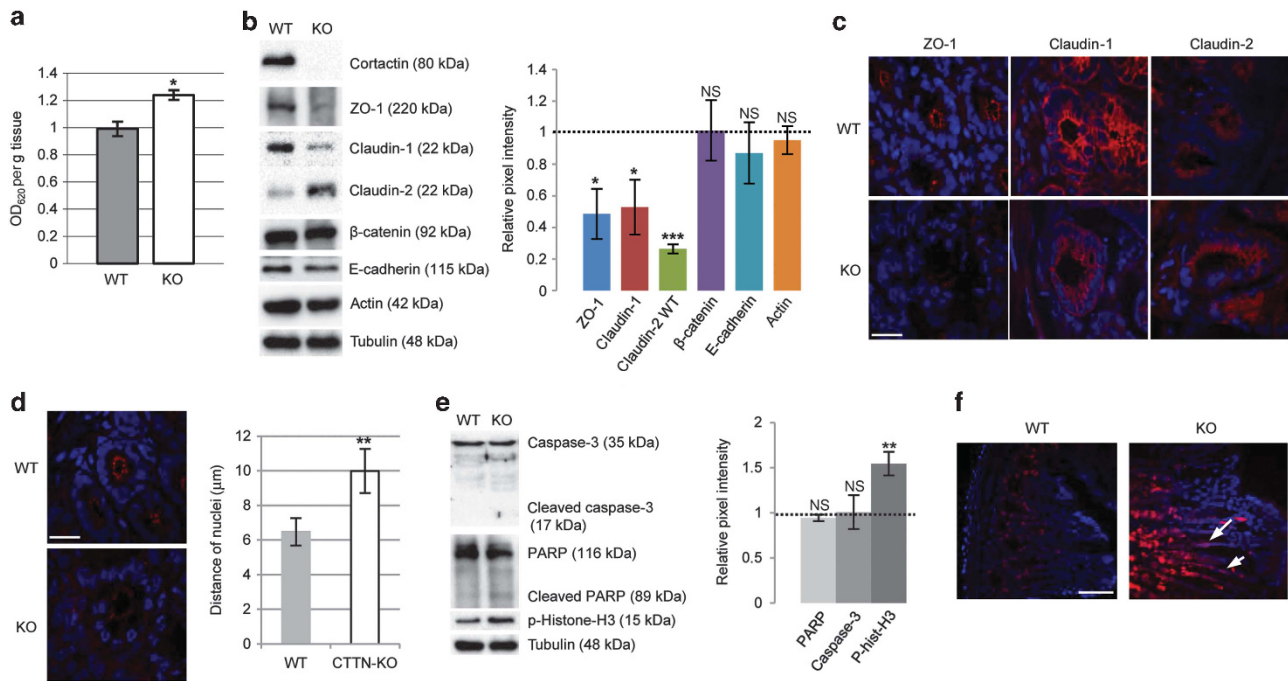


Figure 1 Cortactin deficiency causes increased intestinal epithelial permeability, altered molecular composition of junctions, and crypt deformation. **(a)** Intestinal epithelial permeability to Evan's Blue in wild-type (WT, $n=6$) and cortactin-deficient (KO, $n=8$) mice expressed as absorption per gram tissue. Data are presented as mean \pm s.d.m. * $P<0.05$. **(b)** Western blot analysis of the indicated proteins in colon tissue lysates of WT and KO mice. The bar graph shows mean pixel intensity of KO bands normalized to WT bands that were set to 1 (dotted line). In the case of claudin-2, levels are depicted in a reverse fashion, i.e., mean WT band pixel intensity normalized to KO band intensity (set to 1). All proteins were normalized to tubulin levels. Graph shows quantification from three independent experiments. * $P<0.05$, ** $P<0.001$, NS, not significant. **(c)** Immunofluorescence stainings of ZO-1, claudin-1, and claudin-2 in crypts of WT and KO mice. ZO-1 is shown in red, nuclei in blue. Bar = 20 μ m. **(d)** Absence of cortactin alters crypt morphology as manifested by increased distances between epithelial nuclei. ZO-1 is shown in red, nuclei in blue. Bar = 20 μ m. Graph shows quantification of nuclei distances of 36 crypts from three independent experiments. ** $P<0.01$. **(e)** Cortactin deficiency does not cause cleavage of caspase-3 or poly-(ADP-ribose)-polymerase (PARP) but induces phosphorylation of histone H3. The bar graph shows mean pixel intensity of cortactin KO bands normalized to WT bands that were set to 1 (dotted line). All proteins were normalized to tubulin levels. ** $P<0.01$; NS, not significant. **(f)** Ki67 staining (red) shows proliferating cells along the crypt axis (arrows) in cortactin KO colons, while they are mostly restricted to the crypt base in WT colons. Bar = 50 μ m. All blots and images are representative of three independent experiments.

untreated KO mice displayed minimal signs of inflammation/edema leading to an increased histological score. DSS treatment led to an increased score in WT mice and this increase was more pronounced in KO mice (see **Supplementary Figure S1B**). These tissue alterations likely explain why cortactin KO animals suffer more severely from colitis than WT.

We observed strong mucus deposition in KO colons after DSS treatment. To analyze whether this is a consequence of altered Goblet cell numbers, we performed periodic acid-Schiff stainings (see **Supplementary Figure S2A**). We found that Goblet cell numbers are significantly increased at basal conditions in untreated KO mice, which might constitute a compensatory mechanism to counteract the increased basal epithelial permeability and prevent bacterial translocation (see **Supplementary Figure S2B**). Goblet cell numbers decreased after DSS treatment in WT mice as expected, and decreased even further in the colons of cortactin KO mice after DSS treatment. Additionally, we found that goblet cells are morphologically changed in KO colons after DSS treatment. While WT goblet cells showed a round morphology, cortactin-deficient goblet cells displayed a rather elongated and bigger shape after DSS treatment as demonstrated by a reduced circularity index (see **Supplementary Figure S2A,C**). Given the

observed increased mucus secretion (**Figure 2d**) in KO mice during DSS treatment, these data point to a depletion/exhaustion of Goblet cells in the absence of cortactin during inflammation.

Interestingly, increased proliferation as observed in untreated cortactin KO colon epithelium (**Figure 1f**) was no longer observed after DSS treatment (see **Supplementary Figure S3**). This finding suggests that this potential protective mechanism under basal conditions¹⁸ is no longer active under inflammatory conditions, which could contribute to the more severe phenotype in cortactin KO mice.

Leukocyte recruitment occurs in response to inflammatory stimuli. In WT colons, we observed robust leukocyte recruitment in response to DSS treatment as expected (see **Supplementary Figure S4**). The numbers of both CD45⁺- and CD68⁺ cells were significantly increased (see **Supplementary Figure S4C and D**). Interestingly, the number of CD45⁺ cells was significantly reduced in the colons of cortactin KO mice, whereas the number of CD68⁺ cells was similar to controls (see **Supplementary Figure S4C,D**). Of note, cortactin deficiency prevented the recruitment of both CD45⁺ and CD68⁺ cells into the mucosa in response to DSS treatment, which could be explained by the known defects in leukocyte extravasation.¹⁶

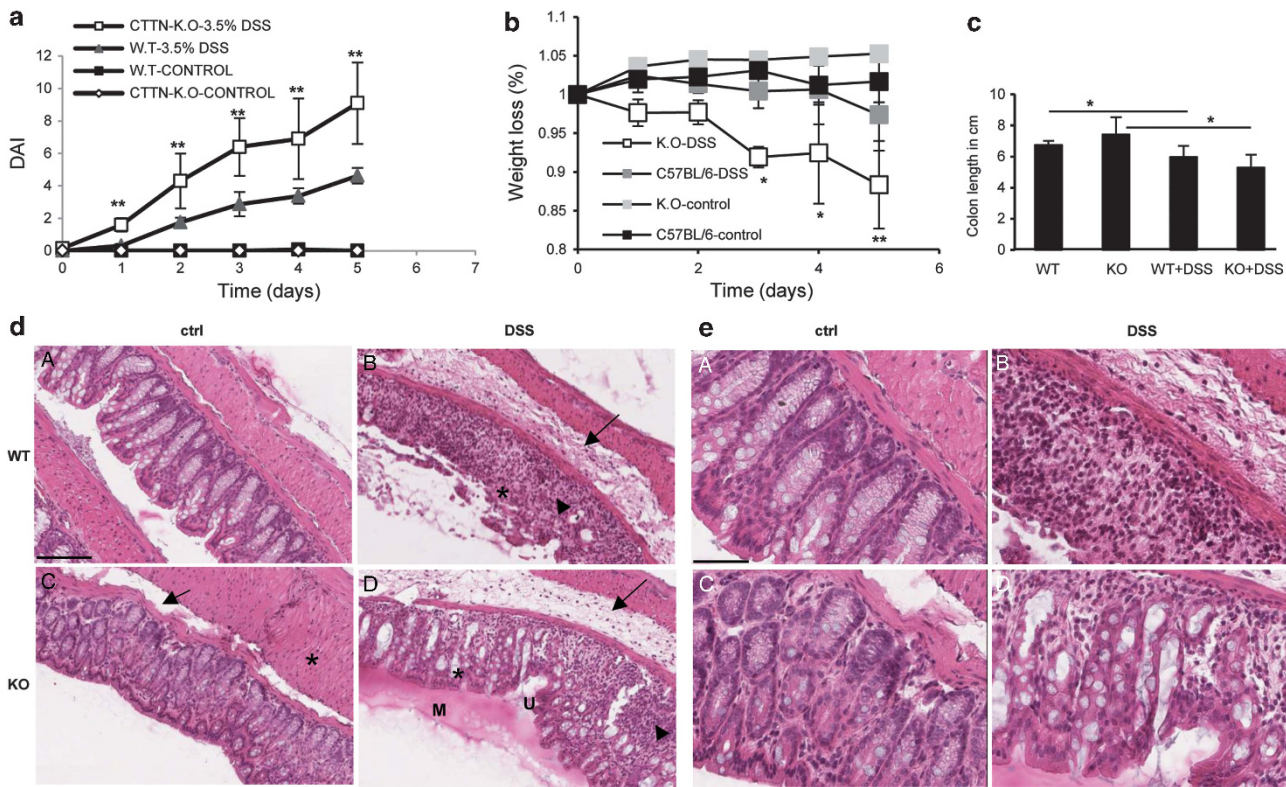


Figure 2 Cortactin-KO mice are more susceptible to dextran sulfate sodium (DSS)-induced colitis. (a) Cortactin-KO mice develop a higher disease activity index (DAI) and start dying after 5 days of DSS treatment ($n=12$ in each group). (b) Cortactin-KO mice lose more weight during DSS colitis ($n=12$). (c) DSS induces colon shortening in both wild type (WT) and KO mice ($n=12$). All data are presented as mean \pm s.d.m. * $P<0.05$; ** $P<0.01$. (d, e) Hematoxylin/eosin-stained distal colon areas in $\times 20$ magnification (d) and $\times 40$ (e) from the respective “swiss rolls” shown in Supplementary Figure S1 (bars = 100 μ m (d), 50 μ m (e)): (A) untreated WT showing normal tissue architecture; (B) DSS-treated WT showing crypt dysplasia and ulceration (*), immune cell infiltration (arrow-head) that extends into the lamina propria, and edema (arrow); (C) untreated KO showing mostly conserved tissue architecture but with light edema formation (arrow) and thickening of the muscularis (*); and (D) DSS-treated KO showing edema formation (arrow), inflammatory cell infiltration (arrow-head), ulceration (U), goblet cell hyperplasia (*), and large mucus deposits (M).

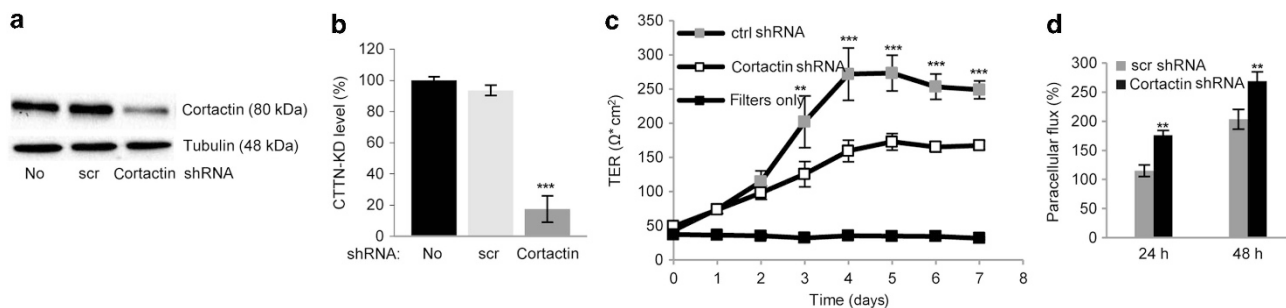


Figure 3 Cortactin depletion causes barrier dysfunction. (a) Transduction of Caco-2 cells with lentiviral constructs expressing cortactin-specific shRNA causes cortactin downregulation. (b) Quantification of blots from three independent cell lysates revealed a significant downregulation of $84.3 \pm 8.7\%$ compared with scrambled control cells (no: Caco-2 cells without lentiviral transduction; scr: Caco-2 cells transduced with a lentivirus expressing a scrambled shRNA). (c) Cortactin-depleted Caco-2 cells develop TER to a lesser extent compared with cells transduced with a scrambled control shRNA. (d) Paracellular flux of 4 kDa FITC-dextran is increased without cortactin. ** $P<0.01$; *** $P<0.001$. Graphs summarize three independent experiments. TER, transepithelial electrical resistance.

Cortactin-depleted Caco-2 cells also show barrier dysfunction under basal conditions

In order to analyze the mechanisms causing barrier dysfunction in the absence of cortactin, we generated stable cortactin-depleted Caco-2 cells using shRNA-expressing lentiviruses (Figure 3a). We achieved a maximal knock-down efficiency of

$84.3 \pm 8.7\%$ (Figure 3b). First, we proved that these cells are an appropriate model resembling the observed *in vivo* effects. As expected, development of transepithelial electrical resistance (TER) was significantly lower in cortactin-depleted cells (Figure 3c), while paracellular flux of 4kDa FITC-dextran was significantly higher without cortactin (Figure 3d).

Cortactin depletion leads to altered junction architecture and increased proliferation

Similar to what we observed *in vivo*, we also detected reduced levels of the TJs proteins ZO-1, occludin, and claudin-1, while the leaky claudin-2 was strongly increased without cortactin (**Figure 4a**). E-cadherin levels were significantly reduced, whereas claudin-4 and β -catenin levels remained unaltered (**Figure 4a**). Immunofluorescence stainings confirmed the western blot data and showed reduction of ZO-1, occludin, and E-cadherin to varying extents, without alterations in β -catenin levels (**Figure 4b**).

Apoptosis was not induced in the absence of cortactin as indicated by absence of poly-(ADP-ribose)-polymerase and caspase-3 cleavage (**Figure 4c**), but we again observed significantly higher phosphorylation levels of histone-H3 pointing to increased proliferation (**Figure 4c**), which is consistent with our observation that cortactin-depleted Caco-2 cells adhered less efficiently but then grew faster in culture and tended to overgrow once a monolayer was established (see **Supplementary Figure S5**). Thus, cortactin-depleted Caco-2 cells are an appropriate model resembling the molecular changes observed in cortactin KO mice.

Absence of cortactin favors ROCK1-dependent stress fiber formation

Interestingly, we consistently observed many more actin fibers crossing cortactin-depleted cells (**Figure 5a**), suggesting that increased actomyosin contractility may contribute to the destabilization of interepithelial junctions.⁴ These fibers appeared mostly in the apical regions where they connected to TJs as demonstrated by a partial colocalization with ZO-1 (see **Supplementary Figure S6**). Moreover, phalloidin stainings of colon tissues revealed a similar increase in actin filaments in the absence of cortactin (see **Supplementary Figure S7**). These fibers also appeared mostly in the apical regions, suggesting that stress fiber-mediated pulling forces contribute to the destabilization of TJs without cortactin. Analyzing the G-actin to F-actin ratio in colons, we indeed found increased levels of F-actin in cortactin KO mice compared with WT littermates that was accompanied by a reduction in G-actin while the total actin concentration was unaffected (**Figure 5b**). Quantification showed a statistically significant shift in F- to G-actin ratios from 0.813 ± 0.069 in the WT to 2.349 ± 0.213 in KO. Given this increase in filamentous actin, we investigated molecules involved in the regulation of

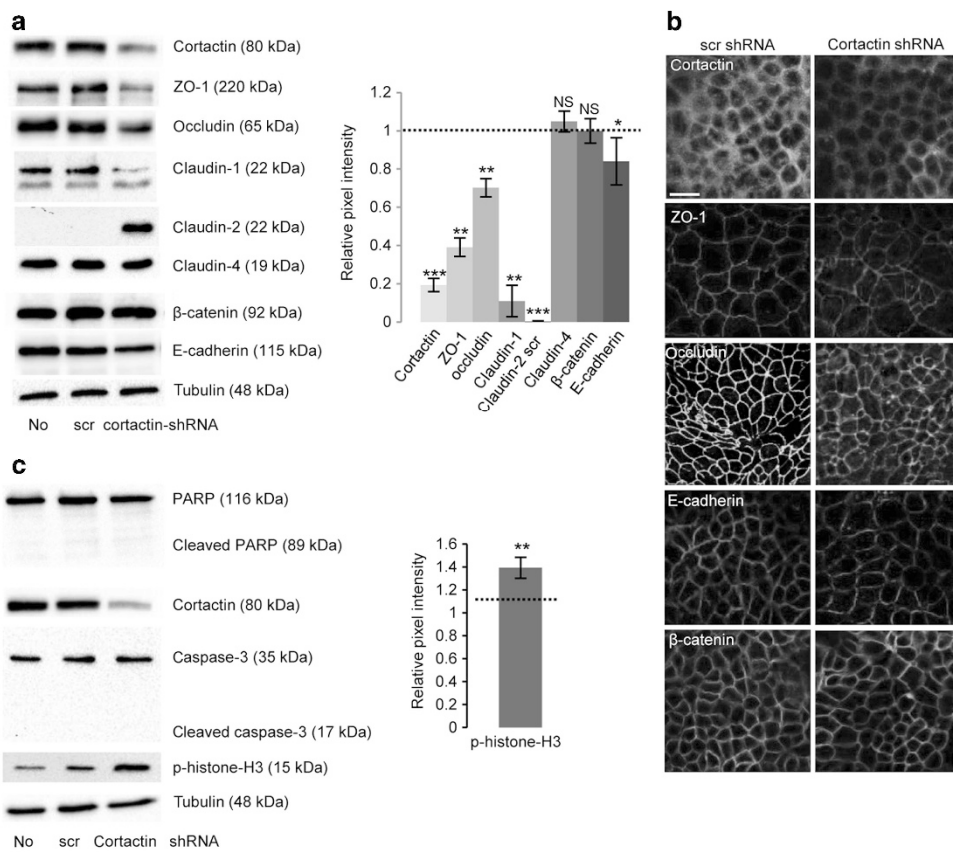


Figure 4 Cortactin depletion leads to altered junction architecture and increased proliferation. **(a)** Western blot analysis of the indicated proteins in the respective Caco-2 lysates. The bar graph shows mean pixel intensity of cortactin shRNA bands normalized to scr shRNA bands that were set to 1 (dotted line). In the case of claudin-2, levels are depicted in a reverse fashion, i.e., mean scr shRNA band pixel intensity is shown normalized to cortactin shRNA band intensity (set to 1). All proteins were normalized to tubulin levels. * $P < 0.05$, ** $P < 0.01$, *** $P < 0.001$; NS, not significant. **(b)** Immunofluorescence stainings of the indicated proteins in the respective Caco-2 monolayers in grayscale. Bar = 20 μ m. **(c)** Cortactin depletion does not cause cleavage of caspase-3 or poly-(ADP-ribose)-polymerase (PARP) but induces phosphorylation of histone H3. The bar graph shows the mean pixel intensity of the p-histone-H3 band from the cortactin shRNA sample normalized to the respective scr shRNA band that was set to 1 (dotted line). ** $P < 0.01$. All blots and stainings are representative of three independent experiments.

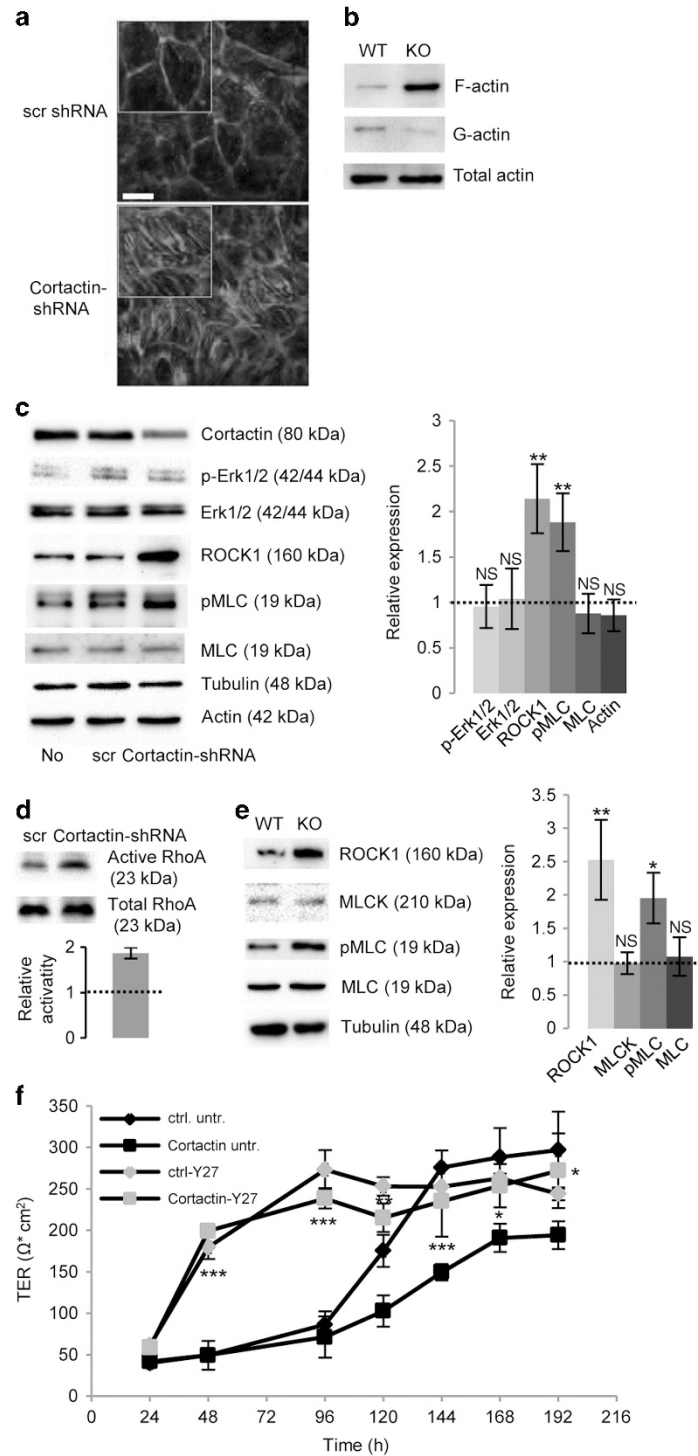


Figure 5 Cortactin depletion causes ROCK1-dependent actomyosin contractility. **(a)** Cortactin-depleted Caco-2 cells show more actin fibers crossing the cell body. Images representative of three independent experiments. Bar = 20 μm . **(b)** Cortactin KO colons have increased F-actin and decreased G-actin levels with total actin levels being unaltered. **(c)** Cortactin depletion does not cause activation of Erk but increases expression of ROCK1 and phosphorylation of myosin light chain (MLC). The bar graph shows mean pixel intensity of cortactin shRNA bands normalized to scr shRNA bands which were set to 1 (dotted line). Proteins were normalized to tubulin levels except for pMLC which was normalized to total MLC expression. ** $P < 0.01$; NS, not significant. **(d)** Representative western blot of total RhoA and active RhoA in cortactin-depleted and control Caco-2 cells after pull-down assays using Rhotekin-GST beads. Quantification of three independent blots is shown below and expressed as relative activity of RhoA in cortactin-shRNA Caco-2 with the scr-shRNA Caco-2 band set to 1 (dotted line). $P = 0.0018$. **(e)** Western blots of mouse colon tissue lysates also show increased ROCK1 expression and MLC phosphorylation in the absence of cortactin without changes in MLCK or total MLC levels. All blots are representative of three independent experiments. The bar graph shows mean pixel intensity of cortactin KO bands normalized to WT bands which were set to 1 (dotted line). All proteins were normalized to tubulin levels except for pMLC which was normalized to total MLC expression. * $P < 0.05$; ** $P < 0.01$; NS, not significant. **(f)** Inhibition of ROCK1 in Caco-2 cells with 10 μM Y27632 rescues the permeability defect in the absence of cortactin. * $P < 0.05$; ** $P < 0.01$; *** $P < 0.001$. Graph summarizes three independent experiments.

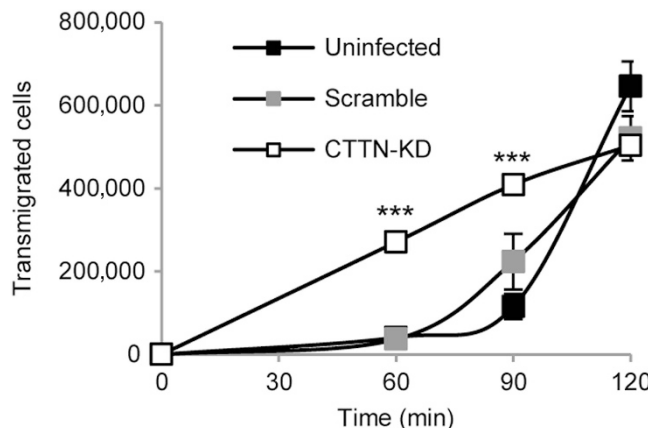


Figure 6 Neutrophils cross a cortactin-depleted Caco-2 monolayer faster. Neutrophils transmigrate faster across cortactin-depleted epithelial monolayers. *** $P<0.001$. Graph summarizes three independent experiments.

actomyosin contractility. We found increased levels of ROCK1 protein that was accompanied by increased phosphorylation of myosin light chain (MLC) (Figure 5c). ROCK1 is activated by RhoA and basal levels of active RhoA were significantly increased in cortactin-depleted Caco-2 cells (Figure 5d). Importantly, ROCK1 expression and MLC phosphorylation were also increased in cortactin-KO colons, whereas MLCK and total MLC levels remained unchanged (Figure 5e), showing that ROCK1-dependent increased actomyosin contractility also occurs *in vivo*. Importantly, treating cortactin-depleted Caco-2 cells with the ROCK1 inhibitor Y27236 rescued the observed defect in TER development in the absence of cortactin over the entire course of the experiment (Figure 5f). We also blotted for activation of Erk1/2 as it is known to be involved in cortactin-mediated signaling.¹⁹ However, we did not detect Erk1/2 activation in cortactin-depleted Caco-2 cells (Figure 5c).

Neutrophils transmigrate faster across cortactin-depleted Caco-2 monolayers

Excessive neutrophil recruitment is another hallmark of IBD.²⁰ To analyze if neutrophils could exploit the weakened epithelial barrier in the absence of cortactin and transmigrate more easily, we performed inverted transwell filter transmigration experiments. Neutrophil transmigration across a cortactin-depleted Caco-2 monolayer occurred more rapidly with most of the neutrophils having crossed the monolayer after 60 and 90 min (Figure 6), suggesting that a cortactin-depleted epithelial monolayer is indeed more permissive for leukocyte transmigration. However, after 2 h, the final number of transmigrated cells was no longer significantly different.

Cortactin is reduced in colon tissues from IBD patients and co-localization with ZO-1 is lost

Finally, we wanted to unravel a potential role for cortactin in the pathogenesis of IBDs. To this end, we analyzed cortactin expression and localization in colon tissue resections of consenting individuals suffering from CD or UC and healthy controls. In healthy tissues, we detected a prominent

localization of cortactin at cell–cell contacts of crypt epithelium in partial co-localization with the TJ protein ZO-1 (Figure 7a, left image). In both CD (Figure 7a, middle) and UC (Figure 7a, right) colon tissues, this co-localization was lost and cortactin accumulated in the cytosol. These localization patterns for both cortactin and ZO-1 were scored for CD (Figure 7b) and UC (Figure 7c) tissue samples as described in Methods. While 100% of healthy control samples had cortactin localization primarily in the cell periphery at intercellular contacts, the pattern shifted toward more cytosolic location of both ZO-1 and cortactin with the latter losing its cell contact location almost completely. We also analyzed human tissue lysates by western blot and found reduced cortactin protein levels in both CD and UC (Figure 7d). Cortactin levels varied among samples as shown in three representative samples in the blot, but quantification of eight independent samples revealed that the reduction of cortactin levels was statistically significant (Figure 7e), implicating that aberrant cortactin expression and localization may play an important role during IBDs.

DISCUSSION

The actin cytoskeleton controls the stability of the intestinal epithelial barrier by supporting the assembly and function of epithelial junctions. Cortical actin filaments connected to junctional proteins are dynamic structures in constant turnover depending on the challenges the barrier faces.²¹ Several actin-binding proteins (ABP) play important roles in actin cytoskeleton remodeling by controlling filament severing and polymerization, thus contributing to junctional integrity.⁸ Until recently, very little was known about the physiological functions of ABP in different tissues. The generation of KO mouse models for various ABP is now starting to fill this gap of knowledge. Our study provides the first *in vivo* evidence that the ABP cortactin is a master regulator of the intestinal epithelial barrier under basal and inflammatory conditions.

We found that cortactin deficiency increased expression of ROCK1, phosphorylation of MLC, and actomyosin contractility, thus causing altered molecular composition of epithelial junctions and increased intestinal epithelial permeability. Increased expression of ROCK1 without cortactin has also been observed by us in endothelial cells where this occurred on the transcriptional level.²² The function of cortactin in the regulation of transcription still remains unexplored mainly because cortactin has no nuclear translocation signal and until recently it has not been detected in the nucleus. In fact, only a recent study demonstrated that acetylated cortactin can localize to the nucleus.²³ In addition to nuclear acetylated cortactin, the observed shift in intracellular F- to G-actin without cortactin (Figure 5b) may affect the levels of nuclear actin that could contribute to altered gene expression and enhanced cell proliferation.

In addition to increased ROCK1 expression, this kinase is also more active as manifested by increased MLC phosphorylation and the fact that cortactin depletion leads to increased activity of RhoA which is a known activator of ROCK1. How cortactin affects basal levels of RhoA activation is currently

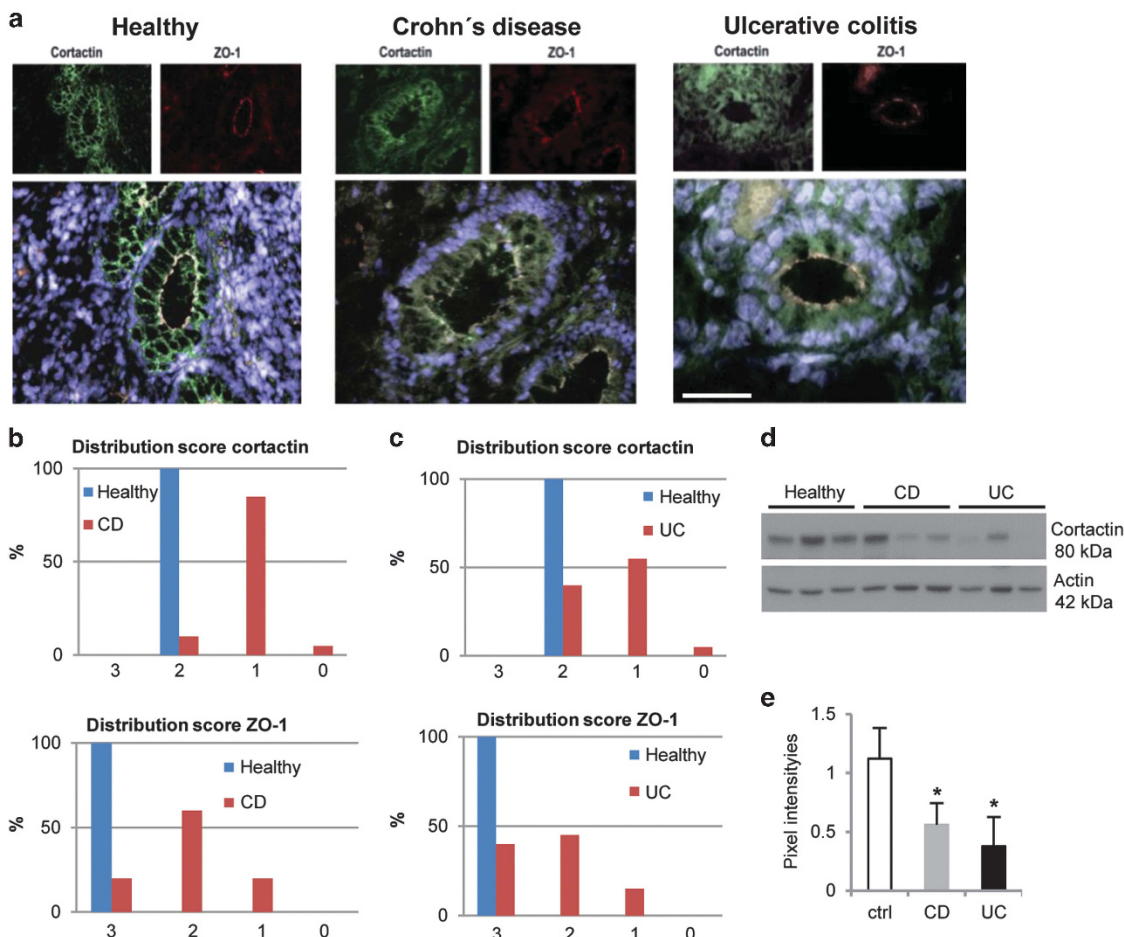


Figure 7 Cortactin is reduced and loses co-localization with ZO-1 at cell contacts in crypt epithelia of colon tissue derived from inflammatory bowel disease patients. (a) Representative Immunofluorescence stainings of cortactin (green) and ZO-1 (red) in crypts of healthy individuals ($n=10$) and individuals suffering from either ulcerative colitis (UC, $n=11$) or Crohn's disease (CD, $n=13$). Bar = 50 μ m. (b) Cortactin (upper graph) and ZO-1 (lower graph) distribution scores in CD tissues evaluated in a blinded fashion as described in the Methods section. (c) Cortactin (upper graph) and ZO-1 (lower graph) distribution scores in UC tissues. (d) Western blot analysis of cortactin protein levels in three different representative colon tissue lysates of each healthy, CD, and UC patients. (e) Graph shows quantification of eight different tissue lysates per condition. Pixel intensities are given as mean \pm s.d.m. * $P<0.05$.

unknown. Therefore, it will be interesting to analyze in future studies whether cortactin interacts with guanine-nucleotide exchange factors or GTPase-activating proteins specific for RhoA to control its activity in epithelial cells.

The increased pulling forces generated by the abundant stress fibers in cortactin-deficient intestinal epithelial cells can certainly contribute to the observed junction disassembly.^{24,25} Destabilization of the intestinal epithelial junctions is further enhanced during DSS colitis in cortactin KO mice leading to an excessive exposure to luminal bacteria and as a consequence to the exaggerated severity of the disease. Such phenomena have also been observed in mice deficient for other ABP such as non-muscle myosin IIA (NMIIA). Mice deficient for NMIIA in the intestinal epithelium also show signs of barrier dysfunction and inflammation under basal conditions but do not develop spontaneous colitis.²⁶ By contrast, ADF-KO mice did not show signs of mucosal inflammation.²⁷ However, similar to cortactin KO mice, both ADF and NMIIA KO develop a much stronger DSS-induced colitis, suggesting that ABP play a general role in protecting from barrier disruption during colitis. The exact

molecular mechanisms of the protective effects of these ABP remain to be examined but likely involve actin-dependent preservation of barrier integrity since inhibition of ROCK1 and thus contractility rescued the permeability increase in cortactin-depleted Caco-2 cells. Interestingly, inhibition of ROCK1 resulted in faster development of TER in both WT and cortactin-depleted cells, suggesting that ROCK1 is a main regulator of epithelial barrier development independently of the presence of cortactin. Even though ROCK-deficient mice exist, they have to the best of our knowledge not been used in colitis experiments.²⁸ RhoA-deficient mice are not viable but floxed mice exist that have been used to create different RhoA-deficient cell types such as fibroblasts, keratinocytes, and macrophages.^{29,30} However, intestinal-specific RhoA KO mice have not been described. Analyzing colitis development using such mice will definitely be an attractive *in vivo* approach to analyze Rho/ROCK signaling in intestinal barrier regulation in the future.

MLC phosphorylation also occurs in response to proinflammatory cytokine-mediated MLCK activation and has also

been observed in IBD patients.²⁴ Although MLC phosphorylation in the absence of cortactin is rather dependent on ROCK1, our data confirm that increased actomyosin contractility contributes to epithelial barrier dysfunction. As mentioned, this phenotype is not sufficient to induce spontaneous colitis, but aggravates DSS colitis. In addition to the described ABP KO mice, this effect has also been observed in transgenic mice overexpressing constitutively active MLCK in intestinal epithelia.³¹ However, in this mouse model, barrier dysfunction was related to mucosal immune activation rather than altered junction architecture. Given the absence of a significant mucosal immune response in the colon that is likely due to the known reduced leukocyte extravasation in the absence of cortactin,¹⁶ cortactin-KO mice thus provide a new model system to study the role of barrier defects for the pathogenesis and progression of experimental colitis without excessive immune activation. It remains unclear why these animals do not get ill despite increased permeability, but this is in agreement with observations made in first-degree relatives of IBD patients that do not develop the disease despite enhanced permeability.^{32,33} Possibilities include, for instance, a differential mucin production pattern as mucin4 deficiency has recently been shown to provide resistance to experimental colitis.³⁴ This is of particular importance since cortactin KO mice respond to DSS treatment with strongly increased mucus deposition (**Figure 2e**). Thus, it will be interesting to analyze the mucin profile in cortactin-KO mice.

We also observed changes in the crypt morphology in the absence of cortactin (**Figure 1d**). As a consequence of increased distances between nuclei without alterations in cell numbers, the crypt lumens appeared bigger in cortactin-deficient colons. Reductions in cell density and contact stability within an epithelial monolayer are known to decrease contact inhibition and as a consequence can induce proliferation.^{35,36} This supports the idea that decreased cell contact stability in the absence of cortactin increases intestinal epithelial cell proliferation *in vivo*. This is also in line with the slight reduction in E-cadherin (**Figure 1b** and **4a**) since E-cadherin levels fine-tune contact-dependent inhibition of proliferation.³⁷ Increased proliferation could also be a mechanism of counteracting the observed barrier dysfunction as increased proliferation can contribute to a regenerative phenotype in the intestinal mucosa.¹⁵

Barrier dysfunction can be exploited by immune cells. *In vitro* transmigration assays showed that neutrophils transmigrated faster across cortactin-depleted Caco-2 monolayers (**Figure 6**). This is in contrast to transendothelial migration that is strongly reduced without cortactin due to failure of intercellular adhesion molecule-1 clustering.^{16,38} In epithelial cells where the direction of transepithelial migration of neutrophils is from the basal to the apical side, the initiation of transmigration is not dependent on intercellular adhesion molecule-1 but instead on other yet to be identified receptors that may not rely on cortactin to cluster around adhering leukocytes. Intercellular adhesion molecule-1 has been shown

to regulate leukocyte–epithelial interactions after transmigration on the apical side.³⁹ It is tempting to speculate that, in addition to easier passage across junctions, cortactin-deficiency prevents this intercellular adhesion molecule-1-dependent adhesive step so that neutrophils are released more rapidly. By contrast, even though cell contacts are destabilized in cortactin KO mice, we did not observe significant leukocyte recruitment as, for example, in junctional adhesion molecule-A -deficient mice.¹⁵ This is in sharp contrast to our observations *in vitro* but can readily be explained by the fact that leukocyte extravasation is reduced in cortactin-deficient mice¹⁶ leading to reduced leukocyte availability in mucosal tissue. However, those immune cells that reach the mucosa could eventually cross the epithelium more easily toward the crypt lumen as suggested by our *in vitro* transmigration assay.

Finally, IBDs patients showed reduced cortactin protein levels in the intestinal epithelium. Furthermore, the co-localization of cortactin with ZO-1 in healthy tissues was mostly lost in tissues from IBDs patients. These alterations in cortactin expression and localization could certainly contribute to barrier dysfunction in these patients. However, whether this is a cause or a consequence of the disease needs to be carefully investigated. Since barrier stability is a prerequisite for healthy intestines, differences in cortactin expression and localization may be a novel risk factor for IBDs. We are not aware of any known cortactin mutations associated with IBDs, but this will also be interesting to analyze in the future.

In conclusion, our data establish cortactin as a critical regulator of intestinal epithelial barrier functions *in vivo* under basal and inflammatory conditions. Manipulating cortactin-dependent functions may therefore be an attractive new approach for the treatment of IBDs.

METHODS

Antibodies and reagents. 4 kDa FITC-dextran and the ROCK inhibitor Y27638 were purchased from Sigma-Aldrich (Toluca, Mexico). The following antibodies have been used: monoclonal anti-cortactin (clone 4F11, 1:3,000; Millipore, Naucalpan, Mexico); anti- γ -tubulin (clone GTU-88, 1:5,000) (Sigma-Aldrich); polyclonal antibodies against ROCK1, MLC, pMLC, ERK, pERK, KI67, and PARP (Cell Signaling, Danvers, MA); polyclonal antibodies against E-cadherin, β -catenin, caspase-3, KI67, p-histone-H3, and species-specific peroxidase-labeled secondary antibodies (1:5,000; Santa Cruz Biotechnologies, Santa Cruz, CA); polyclonal antibodies against claudins-1, -2, and -4, ZO-1, occludin, and species-specific Alexa-labeled secondary antibodies (1:2,000) and Alexa-568-phalloidin (Invitrogen, Carlsbad, CA).

Cell culture. The human IEC line Caco-2 was obtained from ATCC (Manassas, VA) and cultured according to the provided protocols. Generation of a stable cortactin-depleted Caco-2 cell line was performed using the trans-lentiviral packaging kit (Thermo Scientific, Waltham, MA) and the pLKO.1 plasmid (Addgene, Cambridge, MA) according to the manufacturer's instructions. The following sequences have been used: scrambled: CGGAGAAGTGGAGAACATA; cortactin1: CACCAGGAGCATATCAACATA and cortactin2: AAGCTGAGGGAGAATGTCTTT. Cortactin1 shRNA displayed better downregulation efficiencies of 80–90% and has therefore been used in functional experiments.

Western blotting. Equal protein amounts of cell or tissue lysates were separated by SDS-PAGE and transferred electrophoretically to nitrocellulose membranes (Biorad, Mexico-City, Mexico). After blocking unspecific binding sites in TBS containing either 5% skim milk or 2% bovine serum albumin (in case of blots for phosphorylated proteins) for 1 h, membranes were incubated in primary antibodies at 4 °C overnight, washed three times in TBS containing 0.05% Tween-20 for 10 min each, and incubated with species-specific peroxidase-conjugated secondary antibody for 1 h. Chemiluminescence signals were recorded using a ChemiDoc imaging device (Biorad). Tubulin blots were performed as loading controls. Pixel intensities of resulting bands were quantified using ImageJ (NIH, Bethesda, MD).

RhoA activity. Cortactin-depleted and scrambled Caco-2 cells in a 10 cm dish were washed with cold phosphate-buffered saline (PBS) and lysed in 600 µl of a buffer containing 50 mM Tris-HCl, pH7.5, 5 mM EDTA, 150 mM NaCl, 1% TritonX-100, 10 mM MgCl₂, and Complete protease inhibitor cocktail. One hundred microliters of the cell lysates were snap frozen as whole-cell lysate control for the detection of total RhoA. Active RhoA was precipitated from the remaining cell lysate for 1 h at 4 °C using 50 µg Rhotekin-GST (kindly provided by Dr Isaura Meza, Cinvestav, Mexico) bound to glutathione-sepharose. After three washings with cold lysis buffer, levels of RhoA were determined by western blot as described above.

TER and paracellular flux. Transduced Caco-2 cells were plated on 0.4-µm pore size transwell filters (Corning, Monterrey, Mexico) and grown for 48 h. TER of epithelial monolayers was then measured every 24 h using an EVOMX electrovoltmeter with an STX2 electrode (World Precision Instruments, Sarasota, FL). When cells reached a plateau in TER, monolayers were washed three times with HBSS buffer before 10 µl of tracer solution containing 10 µg µl⁻¹ FITC-dextran (MW = 4 kDa; Sigma-Aldrich) in PBS were added to the apical side of monolayers. After 24 and 48 h of incubation at 37 °C, media from the bottom chambers were collected and analyzed fluorometrically (excitation wavelength = 492 nm and emission wavelength = 520 nm).

Neutrophil transepithelial migration. Neutrophil transmigration experiments were performed on 5-µm pore transwell filters (Corning) coated with Attachment factor (Invitrogen) as previously described.⁴⁰ Briefly, human PMNs were isolated from blood of healthy consenting volunteers using Histopaque (Sigma). 1 × 10⁶ cells were added to the upper reservoir and allowed to transmigrate across inverted Caco-2 monolayers (to assure the physiologically relevant direction of transmigration) toward a gradient of 10⁻⁷ M fMLP for 2 h at 37 °C. Transmigrated neutrophils were quantified by assaying for myeloperoxidase as described before.⁴⁰ Transmigration is expressed as the percentage of total applied PMNs per filter.

Mice and DSS colitis. The Institutional Animal Care and Use Committee of Cinvestav approved all mouse experiments. Colitis was induced by 3.5% DSS (40–50 kDa; Affymetrix, Santa Clara, CA) in drinking water in cortactin-deficient¹⁶ or WT littermate control male mice on a C57Bl/6 background within a weight range of 21–25 g. In all experiments, animals received food and water *ad libitum* over a period of 5 days. The disease activity index consisting of weight loss, stool consistency, and perianal bleeding was determined daily as described.⁴¹ After killing the animals by cervical dislocation, colons were removed, its length recorded, and then used in further experiments.

Histology. Paraffin cross-sections or “swiss rolls” of colon tissues were stained with hematoxylin and eosin according to standard protocols. Stained “swiss rolls” were scanned using an Aperio CS2 digital pathology whole image scanner (Leica, Buffalo Grove, IL) and images were analyzed using ImageScope software (Leica). Histological scores were blindly analyzed as described.⁴² Briefly, a score of 0 to 3 for the amount and the extent of inflammation and a score of 0 to 4 for the amount of crypt damage was assigned. These scores were multiplied by

a score for the percentage of tissue involvement: (1) 1–25%; (2) 26–50%; (3) 51–75%; (4) 76–100%.

Immunofluorescence. Caco-2 cells grown to confluence on glass cover slips coated with Attachment factor or 8 µm frozen mouse colon tissue sections or 8 µm frozen resected human colon tissue samples (approved by the Ethic committee of the University Clinic of Münster, Germany) were fixed for 20 min at –20 °C in ethanol and blocked for 1 h in 2% bovine serum albumin and 10% normal goat serum followed by incubation in primary antibodies at 4 °C overnight. Samples were washed and incubated for 1 h with species-specific fluorescently labeled secondary antibodies (Invitrogen). Coverslips were mounted in Vecta-Shield medium containing DAPI (Vectorlabs, Burlingam, CA) and analyzed on a confocal laser microscope (FV-300; Olympus, Miami, FL). Cortactin and ZO-1 distribution scores in stainings of human colon tissue samples were evaluated in a blinded fashion according to the following scheme: 3, staining primarily at cell borders; 2; staining more pronounced at cell borders but also positive in the cytoplasm; 1, staining more pronounced in the cytosol but still positive at cell borders; 0, similar intensities in the cytosol and at cell borders.

G-to F-actin ratio. G/F-actin ratios were analyzed using a G-actin/F-actin *in vivo* assay Biochem kit according to the manufacturer's instructions (Cytoskeleton, Denver, CO).

Permeability assay *in vivo*. Evan's Blue-based *in vivo* colon permeability assays were performed as described.⁴¹ WT and cortactin-KO littermates were anesthetized with an intraperitoneal injection of 125 mg kg⁻¹ ketamine hydrochloride (Sanofi, Mexico-City, Mexico) and 12.5 mg kg⁻¹ xylazine (Phoenix Pharmaceuticals, Burlingame, CA). After laparotomy, a 22G polyethylene tube was inserted into the proximal *colon ascendens* and ligated. Remaining stool was rinsed out, and 1 ml of Evans blue 1.5% (Sigma Aldrich) in PBS was instilled for 15 min. After washing with PBS until the perianal washout was clear, animals were killed and the colon extracted. The colon was opened longitudinally and rinsed again with PBS, followed by 1 ml of 6 mM N-acetylcysteine to remove dye within the mucus. Colons were incubated in 2 ml formamide overnight at room temperature and the extracted dye was measured spectrophotometrically at 610 nm. Values are expressed as arbitrary units per gram tissue.

Statistical analysis. Data are presented as mean with standard deviation of the mean. Statistical significance was assessed using Student's *t*-test and one-way ANOVA with Bonferroni's *post-hoc* test where appropriate. A *P*-value of <0.05 was considered statistically significant.

SUPPLEMENTARY MATERIAL is linked to the online version of the paper at <http://www.nature.com/mi>

ACKNOWLEDGMENTS

We thank Dr Alfonso Felipe López for help with image acquisition and Angelica Silva Olivares for excellent technical assistance. This work was supported by grants of the Mexican Council for Science and Technology (CONACyT, 179895, 207268, and 233395 to Michael Schnoor). A.F.C.M. received a travel fellowship grant from the *Journal of Cell Science*, The Company of Biologists Limited (www.biologists.com). A.F.C.M. and A.G.P. received predoctoral fellowship stipends from Conacyt (346966, 369767, respectively).

AUTHOR CONTRIBUTIONS

A.F.C.M. performed research and statistical analysis, interpreted data, and helped preparing the manuscript; H.V.R. and A.G.P. performed research; M.S.h., A.B., P.N., C.S.L., K.R., and R.M. analyzed and interpreted data; M.S.c. designed and performed research, supervised the study progress, analyzed and interpreted data, and wrote the manuscript. All authors reviewed the manuscript.

DISCLOSURE

The authors declared no conflict of interest.

© 2017 Society for Mucosal Immunology

REFERENCES

- Schmitz, H. et al. Altered tight junction structure contributes to the impaired epithelial barrier function in ulcerative colitis. *Gastroenterology* **116**, 301–309 (1999).
- Shen, L., Weber, C.R., Raleigh, D.R., Yu, D. & Turner, J.R. Tight junction pore and leak pathways: a dynamic duo. *Annu. Rev. Physiol.* **73**, 283–309 (2011).
- Ivanov, A.I. & Naydenov, N.G. Dynamics and regulation of epithelial adherens junctions: recent discoveries and controversies. *Int. Rev. Cell Mol. Biol.* **303**, 27–99 (2013).
- Ivanov, A.I., Parkos, C.A. & Nusrat, A. Cytoskeletal regulation of epithelial barrier function during inflammation. *Am. J. Pathol.* **177**, 512–524 (2010).
- Van Itallie, C.M. & Anderson, J.M. Architecture of tight junctions and principles of molecular composition. *Semin. Cell Dev. Biol.* **36**, 157–165 (2014).
- Meng, W. & Takeichi, M. Adherens junction: molecular architecture and regulation. *Cold Spring Harb. Perspect. Biol.* **1**, a002899 (2009).
- Yonemura, S. Cadherin–actin interactions at adherens junctions. *Curr. Opin. Cell Biol.* **23**, 515–522 (2011).
- Garcia-Ponce, A., Citalan-Madrid, A.F., Velazquez-Avila, M., Vargas-Robles, H. & Schnoor, M. The role of actin-binding proteins in the control of endothelial barrier integrity. *Thromb. Haemost.* **113**, 20–36 (2015).
- Cosen-Binker, L.I. & Kapus, A. Cortactin: the gray eminence of the cytoskeleton. *Physiology (Bethesda)* **21**, 352–361 (2006).
- Helwani, F.M. et al. Cortactin is necessary for E-cadherin-mediated contact formation and actin reorganization. *J. Cell Biol.* **164**, 899–910 (2004).
- Han, S.P. et al. Cortactin scaffolds Arp2/3 and WAVE2 at the epithelial zonula adherens. *J. Biol. Chem.* **289**, 7764–7775 (2014).
- Boguslavsky, S. et al. p120 catenin regulates lamellipodial dynamics and cell adhesion in cooperation with cortactin. *Proc. Natl. Acad. Sci. USA* **104**, 10882–10887 (2007).
- Katsube, T., Takahisa, M., Ueda, R., Hashimoto, N., Kobayashi, M. & Togashi, S. Cortactin associates with the cell-cell junction protein ZO-1 in both *Drosophila* and mouse. *J. Biol. Chem.* **273**, 29672–29677 (1998).
- Lai, F.P. et al. Cortactin promotes migration and platelet-derived growth factor-induced actin reorganization by signaling to Rho-GTPases. *Mol. Biol. Cell* **20**, 3209–3223 (2009).
- Laukoetter, M.G. et al. JAM-A regulates permeability and inflammation in the intestine in vivo. *J. Exp. Med.* **204**, 3067–3076 (2007).
- Schnoor, M. et al. Cortactin deficiency is associated with reduced neutrophil recruitment but increased vascular permeability in vivo. *J. Exp. Med.* **208**, 1721–1735 (2011).
- Anderson, J.M. & Van Itallie, C.M. Physiology and function of the tight junction. *Cold Spring Harb. Perspect. Biol.* **1**, a002584 (2009).
- Gomez-Suarez, M. et al. 14-3-3 proteins regulate Akt Thr308 phosphorylation in intestinal epithelial cells. *Cell Death Differ.* **23**, 1060–1072 (2016).
- Stamatovic, S.M., Sladojevic, N., Keep, R.F. & Andjelkovic, A.V. PDCD10 (CCM3) regulates brain endothelial barrier integrity in cerebral cavernous malformation type 3: role of CCM3-ERK1/2-cortactin cross-talk. *Acta Neuropathol.* **130**, 731–750 (2015).
- Fournier, B.M. & Parkos, C.A. The role of neutrophils during intestinal inflammation. *Mucosal Immunol.* **5**, 354–366 (2012).
- Mehta, S., Nijhuis, A., Kumagai, T., Lindsay, J. & Silver, A. Defects in the adherens junction complex (E-cadherin/ beta-catenin) in inflammatory bowel disease. *Cell Tissue Res.* **360**, 749–760 (2015).
- Garcia Ponce, A. et al. Loss of cortactin causes endothelial barrier dysfunction via disturbed adrenomedullin secretion and actomyosin contractility. *Sci. Rep.* **2016**, srep29003 (2016).
- Ito, A. et al. The subcellular localization and activity of cortactin is regulated by acetylation and interaction with Keap1. *Sci. Signal.* **8**, ra120 (2015).
- Cunningham, K.E. & Turner, J.R. Myosin light chain kinase: pulling the strings of epithelial tight junction function. *Ann. NY Acad. Sci.* **1258**, 34–42 (2012).
- Gomez, G.A., McLachlan, R.W. & Yap, A.S. Productive tension: force-sensing and homeostasis of cell-cell junctions. *Trends Cell Biol.* **21**, 499–505 (2011).
- Naydenov, N.G. et al. Nonmuscle myosin IIA regulates intestinal epithelial barrier in vivo and plays a protective role during experimental colitis. *Sci. Rep.* **6**, 24161 (2016).
- Wang, D., Naydenov, N.G., Feygin, A., Baranwal, S., Kuemmerle, J.F. & Ivanov, A.I. Actin-depolymerizing factor and Cofilin-1 have unique and overlapping functions in regulating intestinal epithelial junctions and mucosal inflammation. *Am. J. Pathol.* **186**, 844–858 (2016).
- Julian, L. & Olson, M.F. Rho-associated coiled-coil containing kinases (ROCK): structure, regulation, and functions. *Small GTPases* **5**, e29846 (2014).
- Konigs, V. et al. Mouse macrophages completely lacking Rho subfamily GTPases (RhoA, RhoB, and RhoC) have severe lamellipodial retraction defects, but robust chemotactic navigation and altered motility. *J. Biol. Chem.* **289**, 30772–30784 (2014).
- Thumkeo, D., Watanabe, S. & Narumiya, S. Physiological roles of Rho and Rho effectors in mammals. *Eur. J. Cell Biol.* **92**, 303–315 (2013).
- Su, L. et al. Targeted epithelial tight junction dysfunction causes immune activation and contributes to development of experimental colitis. *Gastroenterology* **136**, 551–563 (2009).
- Buhner, S. et al. Genetic basis for increased intestinal permeability in families with Crohn's disease: role of CARD15 3020insC mutation?. *Gut* **55**, 342–347 (2006).
- Hollandar, D., Vadheim, C.M., Bretholz, E., Petersen, G.M., Delahunty, T. & Rotter, J.I. Increased intestinal permeability in patients with Crohn's disease and their relatives. A possible etiologic factor. *Ann. Intern. Med.* **105**, 883–885 (1986).
- Das, S. et al. Mice deficient in Muc4 are resistant to experimental colitis and colitis-associated colorectal cancer. *Oncogene* **35**, 2645–2654 (2015).
- Eisenhoffer, G.T. & Rosenblatt, J. Bringing balance by force: live cell extrusion controls epithelial cell numbers. *Trends Cell Biol.* **23**, 185–192 (2013).
- McClatchey, A.I. & Yap, A.S. Contact inhibition (of proliferation) redux. *Curr. Opin. Cell Biol.* **24**, 685–694 (2012).
- Kim, J.H., Kushiro, K., Graham, N.A. & Asthagiri, A.R. Tunable interplay between epidermal growth factor and cell-cell contact governs the spatial dynamics of epithelial growth. *Proc. Natl. Acad. Sci. USA* **106**, 11149–11153 (2009).
- Yang, L. et al. Endothelial cell cortactin coordinates intercellular adhesion molecule-1 clustering and actin cytoskeleton remodeling during polymorphonuclear leukocyte adhesion and transmigration. *J. Immunol.* **177**, 6440–6449 (2006).
- Sumagin, R., Robin, A.Z., Nusrat, A. & Parkos, C.A. Transmigrated neutrophils in the intestinal lumen engage ICAM-1 to regulate the epithelial barrier and neutrophil recruitment. *Mucosal Immunol.* **7**, 905–915 (2014).
- Lee, W.Y., Chin, A.C., Voss, S. & Parkos, C.A. In vitro neutrophil transepithelial migration. *Methods Mol. Biol.* **341**, 205–215 (2006).
- Mennigen, R. et al. Probiotic mixture VSL#3 protects the epithelial barrier by maintaining tight junction protein expression and preventing apoptosis in a murine model of colitis. *Am. J. Physiol. Gastrointest. Liver Physiol.* **296**, G1140–G1149 (2009).
- Dieleman, L.A. et al. Chronic experimental colitis induced by dextran sulphate sodium (DSS) is characterized by Th1 and Th2 cytokines. *Clin. Exp. Immunol.* **114**, 385–391 (1998).